AIP | Journal of Applied Physics

Ion-beam modification of Co/Ag multilayers II: Variation of structural and magnetic properties with Co layer thickness

T. Veres, M. Cai, S. Germain, M. Rouabhi, F. Schiettekatte et al.

Citation: J. Appl. Phys. **87**, 8513 (2000); doi: 10.1063/1.373571
View online: http://dx.doi.org/10.1063/1.373571
View Table of Contents: http://jap.aip.org/resource/1/JAPIAU/v87/i12
Published by the American Institute of Physics.

Ion-beam modification of Co/Ag multilayers II: Variation of structural and magnetic properties with Co layer thickness

T. Veres, M. Cai, S. Germain, M. Rouabhi, F. Schiettekatte, S. Roorda, and R. W. Cochrane[a)]
Département de physique et Groupe de recherche en physique et technologie des couches minces, Université de Montréal, C.P. 6128, Succ. Centre-ville, Montréal, Québec H3C 3J7, Canada

(Received 4 August 1999; accepted for publication 20 March 2000)

The structural, magnetic and transport properties of rf sputtered Co/Ag multilayers with Co-layer thicknesses ranging from 1 to 14 Å have been studied by a combination of x-ray diffraction, magnetic and transport measurements. The magnetoresistance at room temperature has a maximum value of more than 12% for a Co-layer thickness around 5 Å. Magnetic measurements demonstrate that samples near this Co-layer thickness are in the transition region from superparamagnetic to ferromagnetic behavior. X-ray analysis indicates that, during deposition, a significant quantity of Co is dispersed throughout a highly textured Ag matrix. Upon irradiation with 1 MeV Si^+ ions up to a dose of 5×10^{16} Si^+/cm^2, an initial demixing of the Co is followed by segregation into grains with the same texture as the Ag. The resulting changes in the magnetization and magnetoresistance are characterized on the basis of a log-normal distribution of the volume of the magnetic particles. As the particle sizes increase, a systematic evolution towards ferromagnetic behavior for films initially in the superparamagnetic and transition regions results. © *2000 American Institute of Physics.* [S0021-8979(00)08912-X]

I. INTRODUCTION

The relation between giant magnetoresistance (GMR) and spin-dependent scattering at interfaces and in the bulk of magnetic layers is well established in the case of magnetic/nonmagnetic multilayers.[1] However, analysis is more complex in the case of discontinuous multilayers and heterogeneous (alloys/granular) samples in which a small amount of magnetic material (Co, Fe, NiFe, CoFe) is dispersed in a metallic matrix (Cu, Ag). Ferromagnetic, superparamagnetic and spin-glass behavior have been obtained in such materials depending on the distribution in particle sizes, shapes and separations.[2–5]

Existing models describing the GMR and its temperature dependence in heterogeneous materials are based on the assumption of a predominant spin-dependent scattering at the magnetic/nonmagnetic interface. Within this approach, the amplitude of the GMR is controlled by the magnetic-particle surface to volume ratio leading to an inverse proportionality between particle size and GMR.[3,6,7] However, due to the very complex structure of these materials, not all factors affecting the GMR can be readily identified, making the search for good GMR materials a somewhat empirical process.

In the search for conditions appropriate for a significant GMR, various thermal treatments, such as variations in deposition temperatures and postpreparation annealing, have been tried in order to optimize the size, the shape and concentration of the magnetic particles. A successful procedure to control the shape and the concentration of magnetic particles has been proposed by Hylton *et al.*[8] in which discontinuous multilayers were made by annealing sputtered $Ni_{80}Fe_{20}$/Ag multilayers under appropriate conditions. The penetration of the nonmagnetic material (Ag) at the grain boundaries of the NiFe layer results in the formation of flat magnetic particles that promote a multidomain state within the magnetic layer. Discontinuities induced in the magnetic layer are able to promote local antiparallel alignment of the grain moments in adjacent layers due to interlayer interactions.

Several parameters make the Co/Ag system a particularly valuable candidate for studying the effects of a granular structure on the magnetic properties. This system exhibits extremely small equilibrium solid solubility, essentially due to the fact that the surface free energy of Co (2.71 J/m^2) is more than twice that of the Ag (1.30 J/m^2) resulting in a large positive heat of formation between Co and Ag ($\Delta H_m = +26$ kJ/g atom). Coupled with the important lattice mismatch (15%) between fcc Ag and Co, these characteristics ensure a high degree of immiscibility for equilibrium mixtures of these elements. Thermal control of the microstructure of Co/Ag mixtures and its effect on GMR and magnetic properties have been investigated by many authors.[9–13] In general, complex magnetic behavior is found due to the presence of small superparamagnetic and larger ferromagnetic particles and to nonvanishing inter-particle interactions.

Depending on the ion mass, its energy and the dosage, ion-beam irradiation can enhance atomic diffusion, modify crystal structures and alter grain sizes. Moreover, such effects will be strongly dependent on the chemical miscibility between the components so that very different behaviors can be expected depending on the sign of the heat formation.[14–16] Nevertheless, very few studies on the effects produced by ion-beam irradiation in systems exhibiting giant magnetore-

a)Author to whom correspondence should be addressed; electronic mail: cochrane@ere.umontreal.ca

sistance have been reported.[17,18] In an earlier study, we demonstrated a strong reversible decrease of the GMR upon low temperature ion-beam bombardment in Co/Cu multilayers;[19] this decrease could be correlated with the suppression of the interlayer antiferromagnetic coupling under irradiation.

We have recently embarked on a systematic examination of the structural and magnetic modifications from high-energy ion bombardment of sputter-deposited Co/Ag multilayers with Co thicknesses ranging from 2 to 15 Å. In a previous article, Ref. 20, hereafter referred to as article I, we detailed the effects of 1 MeV Si^+ ion irradiation on the multilayer with a Co-layer thickness of 5 Å, for which the magnetoresistance of the as-deposited multilayer is maximum. For this multilayer, it was found that the Co is initially largely dispersed throughout the Ag layers which have a high degree of fcc (111) texture. Upon bombardment, the Co segregates into strongly textured grains, probably also fcc (111) although the x-ray spectra cannot discriminate against hcp (002). The magnetic state evolves from superparamagnetic to mixed superparamagnetic ferromagnetic with a concomitant decrease in the magnetoresistance.

The present article is intended to complement article I by detailing the ion-beam effects on the structure and magnetic properties of multilayers prepared with initial Co-layer thicknesses from 2 to 15 Å. Within this range of thicknesses, the as-deposited Co layers pass from being discontinuous to forming continuous layers, the latter giving rise to superlattice x-ray peaks. The present study focuses on the radiation-induced effects on the size distribution for the Co particles and their influence on the magnetization and magnetoresistance of the samples. In particular, the GMR ratio was found to decrease substantially for the samples close to the transition between the superparamagnetic and ferromagnetic regimes. This degradation is attributed to the decrease in spin-dependent interfacial scattering due to the ion-beam induced phase segregation of the Co particles.

The remainder of this article is divided into three principal sections. In the first, we describe the details of the sample preparation, the magnetic measurements and the ion-beam irradiation. In the second, the structure, transport and magnetic properties of the as-deposited samples are characterized. In the third section, we present the effects of ion-beam irradiation on these same properties as well as an analysis of these effects based on a log-normal size distribution for the Co particles.

II. EXPERIMENTAL DETAILS

Preparation and measurement techniques have been described in article I. Co/Ag multilayers of the form $Ag(50\,Å)/[Co(t_{Co})/Ag(25\,Å)]_{70}$ with t_{Co} ranging from 2 to 15 Å have been prepared on a SiO_2 layer thermally grown on Si (100) substrates by rf triode sputtering. During sputtering, the substrate temperature was maintained at about 40 °C, the sputtering pressure at 4 mTorr of argon (99.999%) and the rf power at 100 W; the resultant sputtering rates were 0.9 Å/s for Co and 5.1 Å/s for Ag.

The crystallographic structure of the samples was investigated using an x-ray diffractometer with a Cu $K\alpha$ source.

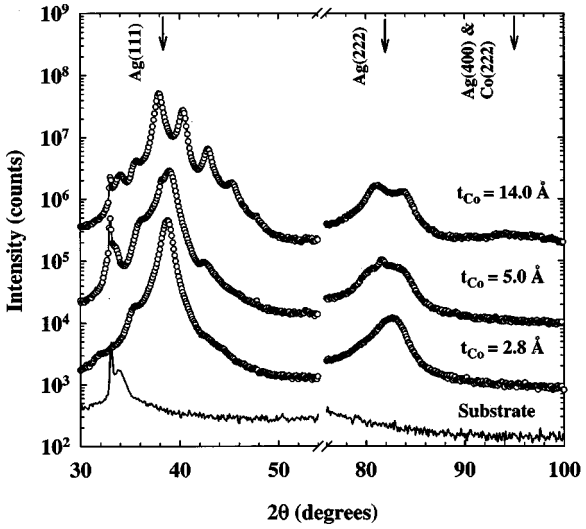

FIG. 1. X-ray diffraction spectra measured using Cu $K\alpha$ radiation for the as-deposited multilayers with $t_{Co}=2.8$, 5.0, and 14 Å. The solid-line spectrum shows the signal originating from the substrate. For clarity, successive spectra have been shifted vertically.

Magnetization curves at room temperature were measured using a vibrating sample magnetometer operating at 85 Hz with a resolution of better than 10^{-5} emu. A number of zero-field cooled (ZFC) and field cooled (FC) magnetization and ac susceptibility runs were made using a modified Quantum Design Model 6000 Physical Property Measurement System. Transport properties (resistivity and anisotropic magnetoresistivity) were obtained by the standard four-point method. Magnetization measurements were taken with the external field applied in the sample plane; magnetoresistance measurements were made for magnetic fields applied in plane (TMR) and perpendicular (PMR) to the plane.

Si^+ ions (1 MeV) from a HV Tandetron accelerator were rastered over a 10×20 mm^2 area at normal incidence in a vacuum of 1×10^{-7} Torr. The ion energy was selected such that its projected range was much greater than the total film thickness (2000 Å) so that a uniform damage profile throughout the multilayer is expected. During irradiation, samples were maintained in thermal contact with a copper block at the liquid-nitrogen temperature and the beam current was kept below 50 nA/cm^2. Each multilayer with configuration $Si/SiO_2/Ag(50\,Å)/[Co(t_{Co})/Ag(25\,Å)]$ ($t_{Co}=2-15$ Å) was irradiated with ion doses ranging from an initial value of 1×10^{13} cm^{-2} to a final value of 5×10^{16} cm^{-2}.

III. AS-DEPOSITED SAMPLES

A. X-ray diffraction

X-ray diffraction spectra for the as-deposited films with $t_{Co}=2.8$, 5.0, and 14 Å are shown in Fig. 1. These data have been chosen because they demonstrate the evolution of the Co-layer structure from dispersed to continuous. Several features should be noted. First, only single phase fcc peaks attributable to (111), (222) planes of Ag and a series of peaks around $2\theta=33°$ arising from the substrate have been observed. Clearly, the polycrystalline grains of all the samples are strongly textured. Moreover, there is no crystallographic

evidence of either fcc or hcp Co in these samples. This conclusion is applicable even for the sample with $t_{Co}=14$ Å since the very broad peak observed around $2\theta=95°$ cannot be simply ascribed to either Ag or Co. In addition, the superlattice peaks observed around the Ag (111) reflection for the film with $t_{Co}=14$ Å as well as the intensity modulation around the Ag (222) peak show that the structural coherence length normal to the film plane is larger than the multilayer period. At a Co-layer thickness of 2.8 Å, the superlattice satellites have completely disappeared indicating a loss of coherence at the interfaces and a degradation of the film layering. At intermediate Co-layer thicknesses (5.0 Å), the superlattice peaks are just barely discernable (see article I).

The fcc Ag (111) peak is generally shifted with respect to the equilibrium bulk position which can be interpreted (article I) as arising from the dispersion of the Co into the Ag layer. This shift depends on the Co-layer thickness. For the sample with $t_{Co}=2.8$ Å, the lattice is contracted by 1.7%. The intensities of the Ag (111) and Ag (222) peaks are larger than those for the other samples, suggesting that for submonolayer thicknesses, the Co atoms form only small clusters or are imbedded into the Ag matrix formed by larger (111) textured grains. For $t_{Co}=5.0$ Å, it was concluded in article I that the double-peaked Ag (111) reflection ($2\theta=38.1°$, $2\theta=39.0°$) was a result of a relatively undeformed Ag buffer layer with a near equilibrium lattice parameter and the remaining multilayer with a significant quantity of the Co dispersed throughout the Ag layer resulting in an average contraction of 2.4%. Finally, for the thickest Co layer (14 Å), the most intense peak is shifted toward lower angles ($2\theta=37.2°$) with respect to the Ag equilibrium position arising from the convolution of the superlattice and atomic periodicities.

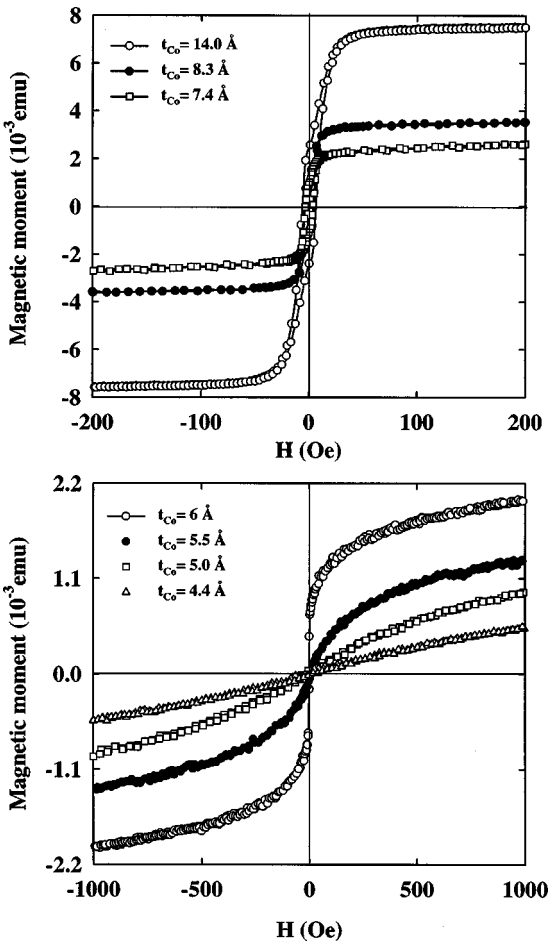

FIG. 2. In-plane magnetization curves measured at room temperature for multilayers with Co thicknesses of 4.4, 5.0, 5.5, 6.0, 7.4, 8.3, and 14 Å.

B. Magnetization

Low-field magnetization curves at room temperature are presented in Fig. 2. For samples with $t_{Co}>7.4$ Å [Fig. 2(a)], the curves demonstrate a ferromagnetic character with small coercivities ($H_c<10$ Oe) and low saturation fields. These samples also show a small in-plane anisotropy. Very different behavior is observed for samples with Co thicknesses below 5.5 Å: the magnetization [Fig. 2(b)] increases linearly through zero at very low applied fields, exhibits no hysteresis and shows little sign of saturation, a superparamagnetic behavior. For intermediate Co-layer thicknesses, the curves display both superparamagnetic and ferromagnetic features testifying to the presence of smaller superparamagnetic Co particles and larger ferromagnetic ones in the as-deposited sample.

As in article I, we analyze the magnetization curves as the sum of two contributions: a superparamagnetic contribution, which requires very large fields for saturation due to the presence of noninteracting small unblocked particles, and a ferromagnetic one arising from larger grains or interacting particles, which is easy to saturate and shows hysteresis. The analysis makes use of the empirical form for the ferromagnetic term employed by Stearns and Cheng[21] cited in article I. This function has been used to fit experimental $M-H$ data using the coercivity H_c, the remanence M_r and the saturation magnetization M^s_{Ferro} as parameters.

To calculate the superparamagnetic contribution, we assume single domain particles above their characteristic blocking temperatures for which the total moment can be described by the Langevin function,[22] $L(x)=\coth(x)-1/x$, $x=\mu(V)H/kT$. Here $\mu(V)=M_sV$ is the magnetic moment of the particle with volume V and saturation magnetization M_s. The superparamagnetic magnetization is then an integral over the volume of the Langevin function weighted by the particle size distribution. This magnetization has a saturation value of M^0_{SP}. We use a log-normal size distribution function of the form[23]

$$f(V)=\frac{1}{\sqrt{2\pi}\,V\sigma}\exp\left[-\frac{(\ln(V/V_m))^2}{2\sigma^2}\right], \tag{1}$$

where σ and V_m, represent, respectively, the half-width and mean value of the size distribution.

Fitting to the magnetization of the as-deposited samples, we find that the ratio $M^s_{\mathrm{Ferro}}/M^0_{\mathrm{SP}}$ between the ferromagnetic and superparamagnetic contributions is near 0 for very thin Co layers, $t_{Co}\leqslant 5$ Å, rising abruptly to 0.44 for $t_{Co}=6$ Å. For Co layers thicker than 8 Å, the samples have almost a pure ferromagnetic behavior. In addition, these fits indicate a systematic increase in the average size of the Co particles; as-

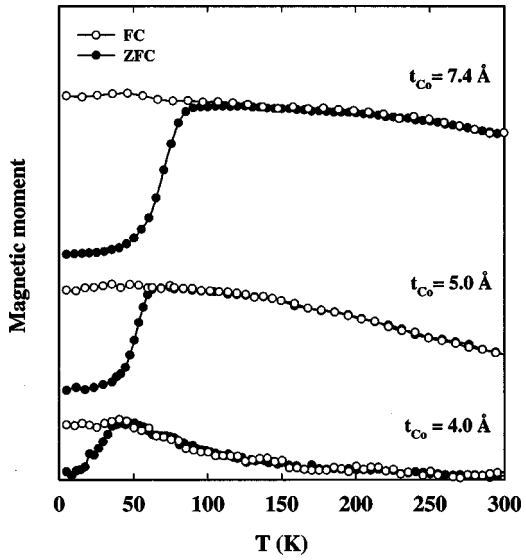

FIG. 3. Temperature dependence of the magnetization measured in an applied field of 20 Oe for the as-deposited multilayers with $t_{Co}=4.0$, Å, 5.0, and 7.4 Å. ZFC (filled circles) and FC (open circles) refer to zero-field-cooled and field-cooled conditions, respectively.

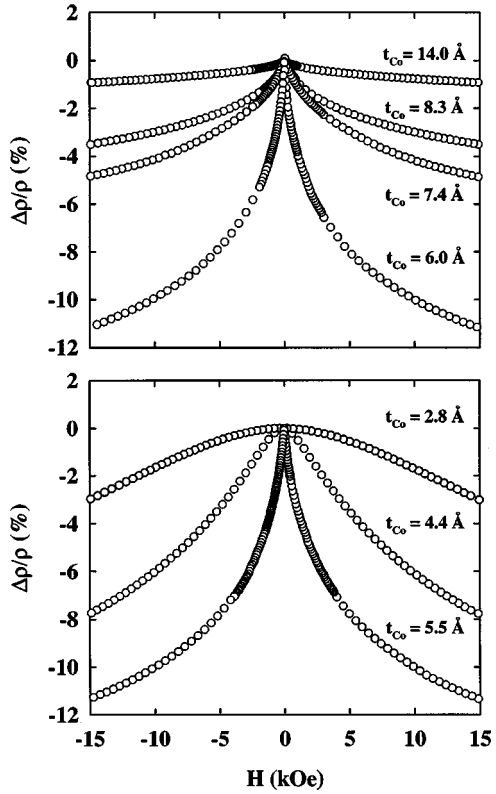

FIG. 4. Room temperature magnetoresistance in transverse geometry for the as-deposited samples with Co thicknesses of 2.8, 4.4, 5.5, 6.0, 7.4, 8.3, and 14 Å.

suming, for simplicity, spherical particles with the volume $V=\pi D^3/6$, the average diameter passes from 32 Å at $t_{Co}=4$ Å to 50 Å at $t_{Co}=6$ Å. These results confirm the conclusions inferred from x-ray measurements that the breakup of the magnetic layer happens at a Co thickness below 7 Å.

Magnetic blocking temperatures are another signature of the superparamagnetic state. Values for the magnetic blocking temperatures of a number of the multilayers were obtained by performing zero-field-cooled (ZFC) and field-cooled (FC) magnetization measurements. ZFC and FC data, measured in a 20 Oe in-plane applied field, are shown in Fig. 3 for three representative samples with Co-layer thicknesses from 4 to 7.4 Å. For $t_{Co}=4$ Å, the peak in the ZFC curve, and the onset of the irreversibility between the FC and ZFC curves indicate an average blocking temperature of 41 K. The blocking temperature rises systematically with Co-layer thickness to 100 K for the sample with Co layers of 7.4 Å.

Considering that the energy barrier to free rotation of the moments of a magnetic particle of volume V can be determined only by the anisotropy energy $E_B=KV$, we can relate this energy to the blocking temperature via the equation[24] $25k_BT_b(H=0)\approx KV$ where $T_b(H=0)$ is the value of the blocking temperature extrapolated to zero field. Taking a value of 4.5×10^5 J/m^3 for the anisotropy constant of fcc Co, the average diameter for the Co particles is estimated (for spherical particles) to range from 35 Å for $t_{Co}=4$ Å to 47 Å when $t_{Co}=7.0$ Å. These values agree reasonably well with those obtained from the analysis of the magnetization curves.

C. Magnetoresistance

Figure 4 is a plot of the room temperature magnetoresistance of a number of the as-deposited multilayers measured in transverse geometry (in-plane magnetic field applied perpendicular to the current). Since the highest available field was 15 kOe, the MR ratio has been defined as $\Delta\rho/\rho_0=[(\rho_{H=0}-\rho_{H=15})/\rho_{H=0}]$, where $\rho_{H=0}$ and $\rho_{H=15}$ are the resistivities in zero and 15 kOe fields, respectively. Very different amplitudes and shapes of the $\rho(H)$ curves are observed as a function of the Co-layer thickness. For $t_{Co}<4$ Å, the MR is relatively small and isotropic and varies very slowly with the applied magnetic field, as is expected for superparamagnetic clusters.

A significant evolution in the MR takes place for Co-layer thicknesses in the range from 5 to 6.5 Å. First, the MR amplitude increases by a factor of 4 compared with that of the thinnest Co layers and the shape of the MR curve changes. Two distinct regions can be identified: in small fields (<3 kOe) the MR decreases rapidly followed by a very slow approach to saturation in larger fields. Beyond a Co-layer thickness of 7.5 Å, the magnitude of the MR falls off rapidly and the variation with field also exhibits a slow approach to saturation. In addition, a significant difference between the in-plane and perpendicular MR curves develops for thick Co layers, suggesting a strong demagnetizing field due to the progressive formation of continuous Co layers.

Even for the sample with the thickest Co layers, the contribution of a ferromagnetic anisotropic magnetoresistance (longitudinal MR minus transverse MR) was small so that the analysis of the MR curves assumes that the scattering originates from small superparamagnetic Co clusters. The field behavior is indicative of a distribution of particle sizes, the larger ones controlling the low field variation and the smaller single-domain particles dominating at high fields.[4,8]

In order to quantify the analysis, we characterize the size distribution of the superparamagnetic particles as log-normal as was done in article I, following the proposal of Gitteleman.[25] Considering that magnetic moments of the particles are randomly oriented, the field dependence of the GMR ratio can be expressed as

$$\frac{\Delta\rho}{\rho}=\frac{\rho(H)-\rho(0)}{\rho(0)}$$
$$=-\alpha_o\cdot\left(\int_{-\infty}^{\infty}L\left(\frac{\mu(V)H}{k_BT}\right)f(V)d(\ln V)\right)^2, \qquad (2)$$

where $\rho(0)$ is zero-field resistivity, $\Delta\rho$ the resistivity change in a field H and α_0 the magnitude of the GMR. The magnetoresistance curves have been fitted using Eq. (2) and a log-normal distribution for the particle sizes described by Eq. (1). The results of this analysis for the as-deposited samples as well as those measured after subsequent irradiation doses are presented in Sec. IV C.

IV. IRRADIATION EFFECTS

In this section we present the effects of ion-beam irradiation on the structure, magnetization and magnetoresistance for samples having different Co thickness.

A. Structural modifications

The evolution of the x-ray structure of the multilayers at all Co-layer thicknesses generally follows that discussed for the film with the 5.0 Å Co-layer thickness detailed in article I. The principal peaks are assigned as Ag (111) around $2\theta=38°$ and Ag (222) near $2\theta=82°$. The initial 2θ positions are several percent higher than the bulk equilibrium values for pure Ag, indicating a lattice contraction resulting from the incorporation of at least part of the Co into the Ag matrix. With ion bombardment, these peaks grow in intensity, narrow and shift almost completely to the bulk positions for pure Ag. In addition, two other peaks emerge at high ion dose ($>2\times10^{15}$ Si^+/cm^2) near $2\theta=43.5°$ and $2\theta=95.5°$ (Fig. 5 and article I). Their positions and the fact that their intensities track the Co-layer thickness leads us to ascribe them to Co (111) and Co (222) reflections, respectively. As with the $t_{Co}=5.0$ Å film studied in article I, the Co grains are highly textured in the same orientation as the Ag grains.

As-deposited multilayers with continuous Co layers exhibit well-developed x-ray superlattice reflections as shown in Figs. 1 and 5. At low doses ($<8\times10^{14}$ Si^+/cm^2), the intensities of the superlattice peaks initially increase as a result of an initial demixing near the interfaces. The superstructure is relatively robust under ion bombardment up to an ion dose exceeding 10^{15} Si^+/cm^2. Larger doses progressively reduce the intensity of the superlattice peaks as the interlayer coherence is destroyed by the breakup of the layer structure and the formation of separate Co and Ag grains.

B. Irradiation effects on the magnetization

Ion-beam irradiation causes significant changes in the magnetization curves. At Co-layer thicknesses of 5 Å and below, the films are initially superparamagnetic at room temperature and only develop a ferromagnetic component upon bombardment, as has been discussed in article I. In the transition zone between Co layers of 5 and 7 Å, a mixed superparamagnetic-ferromagnetic character is present. The evolution of this behavior with ion dose is illustrated in Fig. 6 for the $t_{Co}=6$ Å sample. Extending the analysis described in Sec. III B to the irradiated sample gives at 8×10^{14}

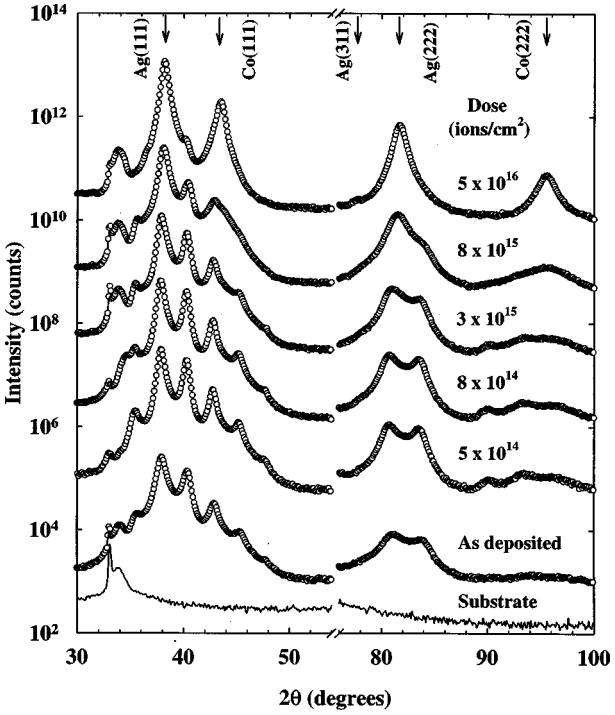

FIG. 5. X-ray diffraction spectra for the 14 Å Co multilayer after various stages of 1 MeV Si^+ irradiation. The substrate signal is represented by the solid-line spectra. Successive spectra have been shifted vertically for clarity.

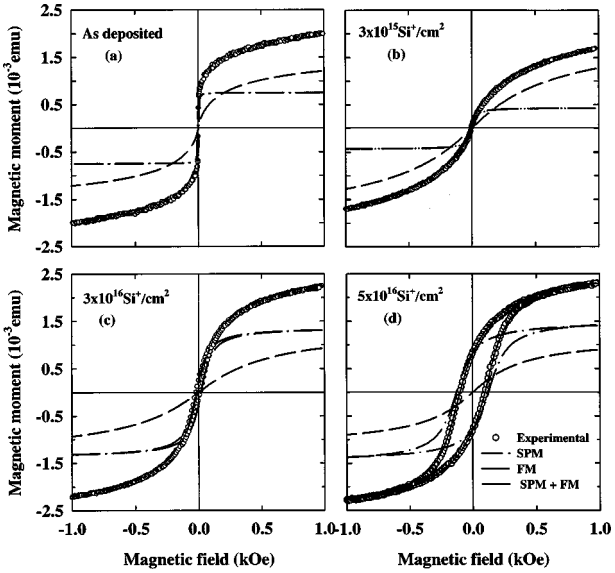

FIG. 6. Magnetization of the $t_{Co}=6.0$ Å sample measured at 300 K after different irradiation doses: (a) as-deposited, (b) 3×10^{15} Si^+/cm^2, (c) 3×10^{16} Si^+/cm^2 and (d) 5×10^{16} Si^+/cm^2. The calculated superparamagnetic (solid) and the ferromagnetic (dashed) contributions are also shown. The total calculated curve (SPM+FM—solid line) is superimposed on the data in (d).

Si^+/cm^2 an initial reduction in the average grain size from $D_m = 48-42$ Å accompanied by a decrease of the ferromagnetic component (M^0_{Ferro}/M_{SP} goes from 0.44 to 0.19). A similar initial decrease in the average grain size has been noted for the 5 Å sample in article I. Subsequent irradiation to 5×10^{16} Si^+/cm^2 almost doubles the average particle diameter to 76 Å leading to a significant conversion of the magnetic material from superparamagnetic to ferromagnetic ($M^0_{Ferro}/M^0_{SP}=1.4$). Details of this evolution under ion bombardment are illustrated in Fig. 6 along with the calculation of the fitted superparamagnetic and ferromagnetic components.

Beyond a Co-layer thickness of about 8 Å (Fig. 2), the film behavior is initially ferromagnetic with a small in-plane anisotropy, characteristic of continuous layers coupled ferromagnetically. Only minor changes can be observed after irradiation up to 3×10^{15} Si^+/cm^2 and, for larger doses, the in-plane magnetization curves become isotropic and the coercive field increases. At all doses, films with thick Co layers maintain a predominantly ferromagnetic character, although there is a rounding of the magnetization curves and a somewhat slower approach to saturation at the highest doses. We conclude that some superparamagnetic clusters are formed as the layers are broken up but that most of the Co remains in grains sufficiently large to support ferromagnetism.

In article I, it was demonstrated that the coercive field H_c increased rapidly at the highest doses for the film with 5 Å Co layers. The same phenomenon occurs for thicker Co layers. At $t_{Co}=6$ Å it is more pronounced but at greater thicknesses the effect is substantially attenuated. In part, this behavior arises from the generation of defects and pinning centers within the films. However, the fact that the variation in H_c is greatest for films in the transition zone from superparamagnetic to ferromagnetic behavior also suggests that it is a consequence of the significant changes in particle sizes, shapes and separations under irradiation. A similar behavior of the coercive field was also observed upon annealing in Co_xCu_{1-x} and Fe_xCu_{1-x} alloys.[26]

C. Irradiation effects on the magnetoresistance

As mentioned in Sec. III C, the magnetoresistance of the as-deposited multilayers varies in magnitude and form with the Co-layer thickness. Under ion bombardment, there are further changes in the MR which differ with t_{Co}. Figure 7 summarizes the behavior of the resistivity and the magnetoresistivity of several representative samples in the series. At all Co-layer thicknesses [Fig. 7(a)], the resistivity ρ increases at least 20% at doses up to about 10^{15} Si^+/cm^2, after which further irradiation causes it to fall to a value close to the original one. In contrast, it can be pointed out that, for Co/Cu multilayers irradiated under similar conditions,[19] the resistivity at high dose continues to increases with ion dose.

The initial increase of the resistivity is the result of several possible factors. On one hand, the x-ray data have shown that ion irradiation initially induces some atomic demixing in the interfacial regions which should normally result in a reduced resistivity; on the other, the irradiation generates bulk defects which have the opposite effect on the resistivity. The universal increase of the resistivity at small doses clearly indicates that defect production has the greater effect. The subsequent decrease in ρ at doses above 10^{15} Si^+/cm^2 is due to the atomic segregation and grain growth; it is apparent that the granular material is less resistive than the corresponding alloy mixture.

Figure 7(b) presents the field induced variation of the resistivity $\Delta\rho$ with ion dose for the samples of Fig. 7(a). For all multilayers, no significant change is observed below a threshold dose of order 10^{15} Si^+/cm^2. With the exception of the thinnest film ($t_{Co}=1.2$ Å), there is a monotonic decrease of $\Delta\rho$ with doses greater than the threshold value; such behavior signals changes in the magnetic disorder on the scale of the mean free path. At the highest dose of 5×10^{16} Si^+/cm^2, $\Delta\rho$ is almost identical for all the samples. Finally, Fig. 7(c) illustrates the variation of the magnetoresistance $\Delta\rho/\rho$ with ion dose. The MR also decreases monotonically, falling quite abruptly beyond the threshold dose for $\Delta\rho$.

Some evolution in the shape of the MR curves is observed, most noticeably for the multilayers with the thinnest Co layers (Fig. 8 for $t_{Co}=2.8$ Å). The initial curve has a parabolic shape with no sign of saturation up to 15 kOe, as is expected for Co dispersed in very small Co clusters. With increasing dose, the shape transforms to a cusp-like form usually observed for GMR materials: the MR drops rapidly at low fields and saturating at a field which decreases with ion dose. For all doses, the MR curves are nearly identical for the field oriented in the sample plane (TMR) and perpendicular to the plane (PMR). This isotropy indicates that the Co particles are reasonably spherical for all ion doses. Application of the analysis of the curves described previously yields quantitative information about the size distribution of the Co particles. For the $t_{Co}=2.8$ Å sample, we calculate an average diameter of 17 Å ($\sigma=0.35$) in the as-deposited sample which rises to 38 Å ($\sigma=0.89$) at the maximum dose of 5×10^{16} Si^+/cm^2.

In the transition region between superparamagnetic and ferromagnetic behavior the shape of the MR curves is cusp-like around $H=0$, as illustrated for $t_{Co}=5.0$ Å in article I. The magnitude of the MR falls in accordance with Fig. 7 as ion irradiation causes growth of the magnetic clusters. Fitting the MR curves reveals that average particle diameters double under ion bombardment: 23–52 Å for $t_{Co}=5.0$ Å (article I); 26–59 Å for $t_{Co}=6.0$ Å. For the as-deposited samples, the analysis of the magnetization curves gives somewhat larger values, but the two analyses converge to very similar values at large ion doses. Nevertheless, both magnetic and transport data support a consistent picture that ion bombardment results in the segregation and growth of the magnetic particles.

For multilayer with $t_{Co}>8$ Å the Co layers are almost continuous. The MR is small and displays anisotropies for field orientations within the plane of the sample and perpendicular to it. Ferromagnets normally exhibit an anisotropic magnetoresistance (AMR) for the field oriented parallel or perpendicular to the current; such an effect is evident for the $t_{Co}=14$ Å film. Upon irradiation the MR and AMR change but never exceed a value of 1%. Furthermore, at high doses, the PMR (field directed perpendicularly to the film surface)

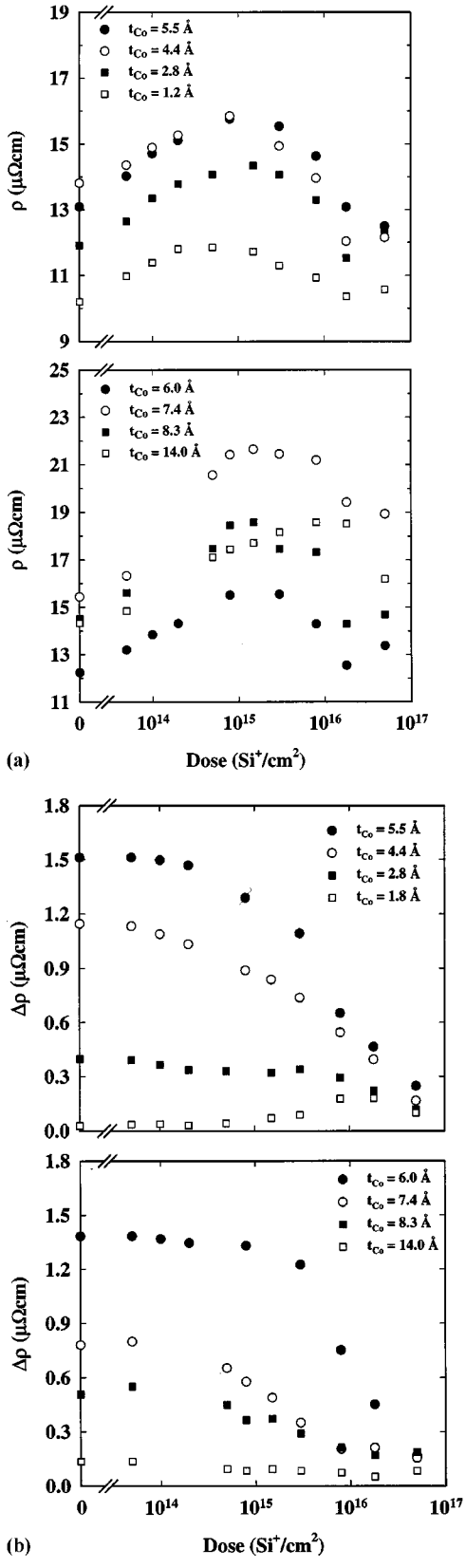

FIG. 7. (a) Resistivity, (b) resistivity change $[\rho(15\ \text{kOe})-\rho(0)]$ and (c) magnetoresistivity at 300 K vs the ion dose for samples with t_{Co} ranging from 1.2 to 14 Å.

is characterized by a demagnetization field which is significantly larger than found for the in-plane MR. It would appear that, even at a dose of 5×10^{16} Si^+/cm^2, the initially continuous Co layers have been broken into quite anisotropic magnetic clusters. As was the case for the magnetization data, the magnetoresistance curves for such thick films cannot be analyzed within the model used for the superparamagnetic samples, so no detailed information is available on the size distribution of the magnetic clusters for these materials.

The decrease of $\Delta\rho$ and $\Delta\rho/\rho$ upon irradiation can be understood if one considers that the spin-dependent scattering at the surface of particles is dominant, as proposed by

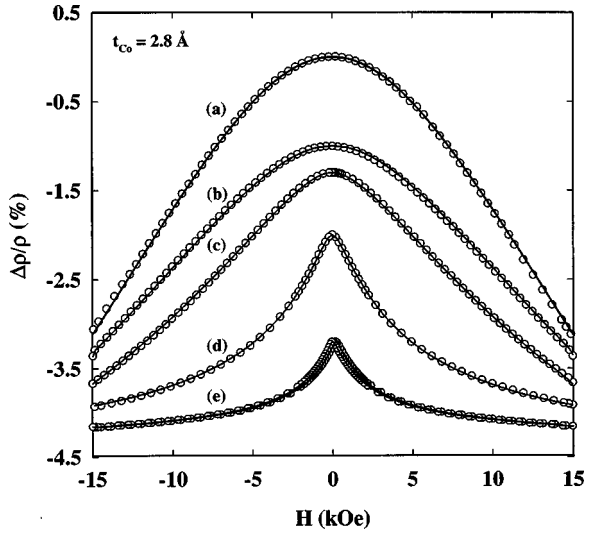

FIG. 8. Field dependence of the transverse magnetoresistance at 300 K for the $t_{Co}=2.8$ Å multilayer at the following ion doses: (a) as-deposited, (b) 5×10^{14} Si^+/cm^2, (c) 3×10^{15} Si^+/cm^2, (d) 1×10^{16} Si^+/cm^2, (b) 5×10^{16} Si^+/cm^2. Solid lines are fits to the data using Eq. (2).

Berkowitz,[2] Zhang and Levy.[6] With this assumption, their models predict that $\Delta\rho$ will decrease as the particle diameter increases since the corresponding reduction in the *surface/volume* ratio results in relatively less spin-dependent interfacial scattering relative to scattering processes in the bulk of the clusters. Qualitatively, it has been noted that the MR falls strongly as the average particle size grows upon irradiation. This effect is demonstrated quantitatively in Fig. 9 where it is shown that the total change in the fitted resistivity varies inversely with the mean magnetic particle size for samples with a significant superparamagnetic component. In the figure, $\Delta\rho$ for the $t_{Co}=5.0$ Å sample is substantially bigger than that found for the $t_{Co}=2.8$ Å film at the same mean cluster size, indicating a dependence on the mean separation of the clusters. Furthermore, for the samples in the transition region (4 Å$<t_{Co}<$7.5 Å), $\Delta\rho$ is somewhat larger than expected on the basis of a collection of superparamagnetic particles only. This difference can be ascribed to contributions from other mechanisms such as reported by Hylton *et al.* in NiFe/Ag multilayers.[8]

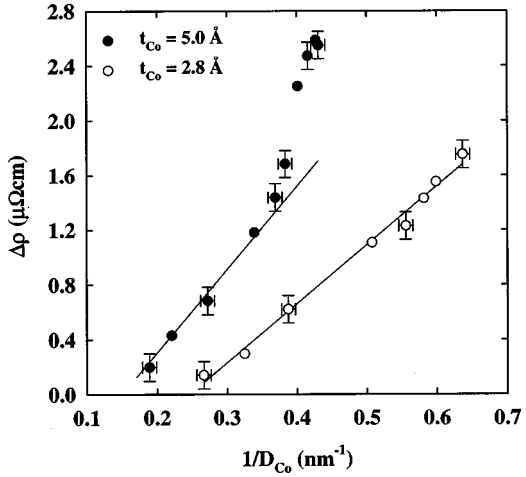

FIG. 9. Maximum change of the fitted resistivity ($\Delta\rho=\alpha_0$) for samples $t_{Co}=2.8$ and 5.0 Å as a function of the inverse mean particle radius. The solid line is a linear fit to the data.

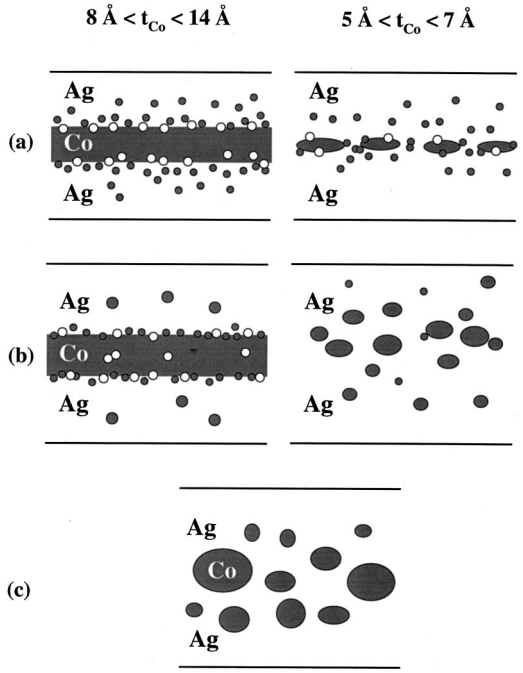

FIG. 10. Schematic representation for the structural evolution upon irradiation: (a) as-deposited, (b) $<1\times10^{15}$ Si^+/cm^2, (c) $>1\times10^{16}$ Si^+/cm^2.

V. CONCLUSIONS

This article completes a study, begun in article I, of the structural, magnetic and transport properties of a series of $[Co(t_{Co})/Ag(25\,Å)]_{70}$ multilayers with Co-layer thicknesses between 2 and 14 Å and their modification by 1 MeV Si^+ ion bombardment. The multilayers can be classified into three groups according to t_{Co}: below about 4 Å, the Co is initially dispersed in the highly textured Ag matrix; above 8 Å a continuous Co layer is formed during deposition; a transition region exists between these values.

Figure 10(a) presents a schematic representation of the structure for the as-deposited multilayers in the transition region (5 Å$<t_{Co}<$ 7 Å), and for the multilayers with continuous Co layers ($t_{Co}>8$ Å).

The large structural changes that we observed upon irradiation are depicted in Fig. 10(b). Low ion doses induce a limited demixing of the elements which is most noticeable for thick continuous Co layers as a sharpening of the superlattice modulation. At high ion doses, the Co is progressively segregated from the Ag. The general tendency to form a granular structure after high dose irradiation is illustrated in Fig. 10(c). The lattice constant of the Ag matrix shows that there is almost a complete phase separation after irradiation by 5×10^{16} Si^+/cm^2. For samples with thin and intermediate Co layers, ion irradiation leads to a systematic growth of Co clusters; for multilayers with initially continuous Co layers, the periodic superstructure is destroyed and the films take on

a granular structure. In all cases, the Co and Ag grains formed after intense ion bombardment share a high degree of structural texturing, essentially fcc (111).

The initial magnetic state of the films varies from superparamagnetic to ferromagnetic for increasing Co-layer thickness. As the samples are irradiated, the magnetic behavior becomes more ferromagnetic as the particles increase in size and become magnetically coupled. The magnetization curves were analyzed to separate superparamagnetic and ferromagnetic components on the basis of their field dependencies up to $t_{Co}=8$ Å; beyond this value the superparamagnetic component is too small for reliable analysis. Mean superparamagnetic cluster diameters increase by about a factor of 2 up to the maximum ion dose of 5×10^{16} Si^+/cm^2.

The magnetoresistance of the as-deposited samples is maximum in the transition region (4.5 Å$<t_{Co}<$6.5 Å); it decreases systematically under ion bombardment for all films beyond a threshold dose of about 10^{15} Si^+/cm^2. Clearly, the largest GMR ratios can be associated with superparamagnetic clusters of a certain size and separation; the GMR becomes negligible with the increase of the mean cluster size and the onset of collective ferromagnetic-like behavior. Fitting the MR curves to a log-normal distribution, as was done for the magnetization, the mean size of the magnetic clusters and their distribution were determined at different irradiation stages. We find that the width and the mean value of the distribution largely increase with irradiation showing that the fraction of large particles, not contributing to the magnetoresistance, is enhanced. The fit shows that $\Delta\rho\propto1/D_m$ for the samples with granular-like behavior consistent with a dominant spin-dependent scattering that occurs mostly at Co/Ag interfaces.

The evolution of the structural, magnetic and transport properties of these Co/Ag samples can be understood on the basis of the mechanisms generally invoked to describe ion-beam mixing in multilayers: collisional (ballistic) transport, thermal spike diffusion and irradiation enhanced diffusion.[27,28] For systems with a large positive heat of mixing, the initial ballistic mixing is partially recovered by chemically driven relocation within cascades which acts as a demixing mechanism in the thermal spike stage of the collision cascade. The role of the chemical driving forces will be enhanced for high doses once atomic relocations over extended regions due to the spatial superposition of cascades begin to promote phase segregation and the agglomeration of neighboring grains.

ACKNOWLEDGMENTS

The authors would like to thank D. Ryan and L. Cheng of McGill University for access to the low temperature magnetometer and for help with the x-ray measurements. It also is a pleasure to acknowledge G. Rinfret and R. Rinfret for their help with the maintenance of the sputtering and magnetoresistance experiments as well as P. Bérichon and R. Gosselin with the operation of the tandetron accelerator. The authors acknowledge the financial support of this research from NSERC of Canada and Le Fonds FCAR du Quebec.

[1] M. N. Baibich, J. M. Broto, A. Fert, F. Nguyen van Dau, F. Petroff, P. Etienne, G. Creuzet, A. Friederich, and J. Chazelas, Phys. Rev. Lett. **61**, 2472 (1988).
[2] A. Berkowitz, A. P. Young, J. R. Mitchell, S. Zang, M. J. Carey, F. E. Spada, F. T. Parder, A. Hutten, and G. Thomas, Phys. Rev. Lett. **68**, 3745 (1992).
[3] J. G. Xiao, J. S. Jiang, and C. L. Chien, Phys. Rev. Lett. **68**, 3749 (1992).
[4] O. Redon, J. Pierre, B. Rodmacq, B. Mevel, and B. Dieny, J. Magn. Magn. Mater. **149**, 398 (1995).
[5] B. Dieny, S. R. Teixeira, B. Rodmacq, C. Cowache, S. Auffret, O. Redon, and J. Pierre, J. Magn. Magn. Mater. **130**, 197 (1994).
[6] S. Zhang, Appl. Phys. Lett. **61**, 1855 (1992); S. Zhang and P. Levy, J. Appl. Phys. **73**, 5315 (1993).
[7] T. A. Rabedeau, M. F. Toney, R. F. Marks, S. S. P. Parkin, R. F. C. Farrow, and G. R. Harp, Phys. Rev. B **48**, 16810 (1993).
[8] T. L. Hylton, K. R. Coffey, M. A. Parker, and J. K. Howard, Science **261**, 1858 (1992).
[9] W. H. Flores, S. R. Teixeira, J. Geshev, J. B. M. da Cunha, P. J. Schilling, A. Traverse, and M. C. Martins Alves, J. Magn. Magn. Mater. **188**, 17 (1998).
[10] A. D. Viegas, J. Geshev, L. S. Dorneles, J. E. Schmidth, and M. Knobel, J. Appl. Phys. **82**, 3047 (1997).
[11] J. R. Regnard, C. Revenant-Brizard, B. Dieny, B. Mevel, and J. Mimault, Mater. Res. Soc. Symp. Proc. **400**, 329 (1996).
[12] J. F. Gregg, S. M. Thompson, S. J. Dawson, K. Ounadjela, C. R. Staddon, J. Hamman, C. Fermon, G. Saux, and K. O'Grady, Phys. Rev. B **49**, 1064 (1994).
[13] L. F. Schelp, G. Tosin, M. Carara, M. N. Baibich, A. A. Gomes, and J. E. Schmidt, Appl. Phys. Lett. **61**, 1858 (1992).
[14] B. M. Paine and R. S. Averbach, Nucl. Instrum. Methods Phys. Res. B **7/8**, 666 (1985).
[15] A. C. Sosa, P. Schaaf, W. Bolse, K. P. Lieb, M. Gimbel, U. Geyer, and C. Tosello, Phys. Rev. B **53**, 14795 (1996).
[16] J. Pacaud, G. Gladyszewski, C. Jaouen, A. Naudon, Ph. Goudeau, and J. Grilhé, J. Appl. Phys. **73**, 2786 (1993).
[17] H. U. Krebs, Y. Luo, M. Störmer, A. Crespo, P. Schaaf, and W. Bolse, Appl. Phys. A: Mater. Sci. Process. **61**, 159 (1995).
[18] V. Kornievski, K. V. Rao, D. M. Kelly, I. K. Shuller, K. K. Larsen, and J. Bøttiger, J. Magn. Magn. Mater. **140–144**, 549 (1995); D. M. Kelly, I. K. Shuller, V. Kornievski, K. V. Rao, K. K. Larsen, J. Bøttiger, E. M. Gyorgy, and R. B. van Dover, Phys. Rev. B **50**, 3481 (1994).
[19] M. Cai, T. Veres, S. Roorda, R. W. Cochrane, R. Abdouche, and M. Sutton, Mater. Res. Soc. Symp. Proc. **504**, 197 (1998).
[20] T. Veres, M. Cai, S. Roorda, and R. W. Cochrane, J. Appl. Phys. **87**, 8494 (2000).
[21] M. B. Stearns and Y. Cheng, J. Appl. Phys. **75**, 6894 (1994).
[22] C. L. Chien, J. Appl. Phys. **69**, 5267 (1991).
[23] R. W. Chantrell, J. Popplewell, and S. W. Charles, IEEE Trans. Magn. **14**, 975 (1978).
[24] B. D. Cullity, *Introduction to Magnetic Materials* (Addison–Wesley, Reading, MA, 1972), p. 410.
[25] J. I. Gitteleman, Y. Goldstain, and S. Bosowski, Phys. Rev. B **5**, 360 (1972).
[26] J. R. Childress and C. L. Chien, J. Appl. Phys. **70**, 5885 (1991); Appl. Phys. Lett. **56**, 95 (1991).
[27] W. L. Johnson, Y. T. Cheng, M. Van Rossum, and M.-A. Nicolet, Nucl. Instrum. Methods Phys. Res. B **7/8**, 657 (1985).
[28] P. Sigmund and A. Gras-Marti, Nucl. Instrum. Methods **182/183**, 25 (1981).